ELSEVIER

Chemistry & Biology 8 (2001) 47–58

Chemistry & Biology

www.elsevier.com/locate/chembiol

Research Paper

The tethered agonist approach to mapping ion channel proteins – toward a structural model for the agonist binding site of the nicotinic acetylcholine receptor

Lintong Li [a], Wenge Zhong [a], Niki Zacharias [a], Caroline Gibbs [a], Henry A. Lester [b], Dennis A. Dougherty [a,*]

[a] *Division of Chemistry and Chemical Engineering, California Institute of Technology, Pasadena, CA 91125, USA*
[b] *Division of Biology, California Institute of Technology, Pasadena, CA 91125, USA*

Received 14 July 2000; revisions requested 21 September 2000 revisions received 27 October 2000; accepted 30 October 2000
First published online 19 December 2000

Abstract

Background: The integral membrane proteins of neurons and other excitable cells are generally resistant to high resolution structural tools. Structure–function studies, especially those enhanced by the nonsense suppression methodology for unnatural amino acid incorporation, constitute one of the most powerful probes of ion channels and related structures. The nonsense suppression methodology can also be used to incorporate functional side chains designed to deliver novel structural probes to membrane proteins. In this vein, we sought to generalize a potentially powerful tool – the tethered agonist approach – for mapping the agonist binding site of ligand-gated ion channels.

Results: Using the in vivo nonsense suppression method for unnatural amino acid incorporation, a series of tethered quaternary ammonium derivatives of tyrosine have been incorporated into the nicotinic acetylcholine receptor. At three sites a constitutively active receptor results, but the pattern of activation as a function of chain length is different. At position α149, there is a clear preference for a three-carbon tether, while at position α93 tethers of 2–5 carbons are comparably effective. At position γ55/δ57 all tethers except the shortest one can activate the receptor. Based on these and other data, a model for the receptor binding site can be developed by analogy to the acetylcholine esterase crystal structure.

Conclusion: Through the use of nonsense suppression techniques, the tethered agonist approach has been made into a general tool for probing receptor structures. When applied to the nicotinic receptor, the method places new restrictions on developing models for the agonist binding site.

Keywords: Tethered agonist; Nicotinic acetylcholine receptor; Agonist binding site; Unnatural amino acid mutagenesis

1. Introduction

The integral membrane proteins of neurons and other excitable cells are generally resistant to high resolution structural tools such as X-ray crystallography and nuclear magnetic resonance (NMR), making efforts to develop mechanistic insights into their function especially challenging. Among the most useful approaches has been the combination of site-directed mutagenesis and electrophysiology, which allows systematic structure–function studies. Recently, this capability was greatly enhanced [1,2] by the adaptation of the nonsense suppression methodology for unnatural amino acid incorporation [3–5] to the heterologous expression system of the *Xenopus* oocyte. To date, over 60 unnatural amino acids have been incorporated into neuroreceptors and ion channels expressed in living cells.

An appropriate target for such studies is the nicotinic acetylcholine receptor (nAChR, Fig. 1). The nAChR family of ligand-gated ion channels underlies transmission at the nerve–muscle synapse and in the autonomic and central nervous system [6–8]. It also serves as the target for nicotine and a number of promising pharmaceuticals for pain, memory enhancement, and the treatment of Parkinson's disease.

Abbreviations: ACh, acetylcholine; nAChR, nicotinic acetylcholine receptor; TMB-8, (diethylamino)octyl 3,4,5-trimethoxybenzoate; AChE, acetylcholine esterase

* Correspondence: Dennis A. Dougherty;
E-mail: dad@igor.caltech.edu

1074-5521/01/$ – see front matter
PII: S1074-5521(00)00055-7

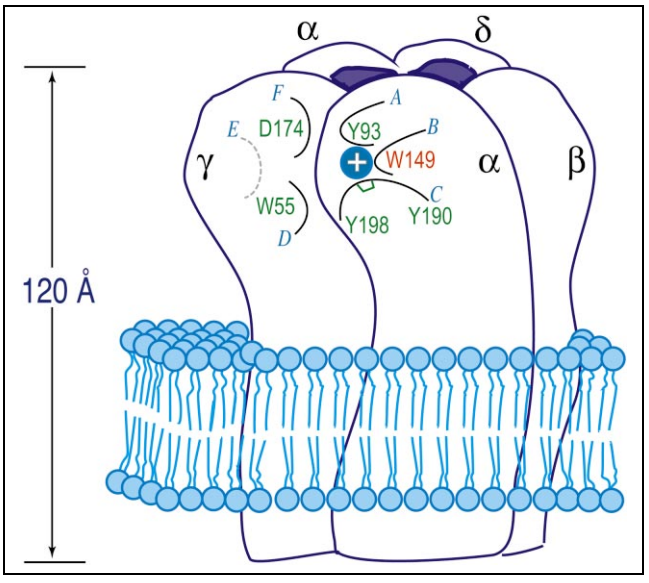

Fig. 1. Structural aspects of the nAChR. The global structure is based on the cyroelectron microscopy of Unwin [9], but with an alternative arrangement of subunits favored by many [10]. Superimposed on the structure are the multiple 'loops' thought to contribute to the agonist binding site (blue circle with positive charge), with key residues identified. The loop image is an adaptation of a model first presented by Changeux [11]. Loops A, B, and C are considered the 'principal components' of the agonist binding site, while D, E, and F are considered 'complementary'. Loop E is only implicated in binding curare, not ACh, but is shown here for consistency with other schemes. Trp α149 is highlighted as the established cation–π binding site for ACh [12]. The 'bracket' on loop C represents the disulfide between C192 and C193, one of the first regions established to be near the agonist binding site [13]. The δ subunit contains residues that are analogous to those shown on the γ subunit (Trp δ57 and Asp δ180), which contribute along with the other α subunit to the second agonist binding site [14]. This is a highly schematic image, as the absolute and relative positions of the loops on the receptor structure remain unknown.

We are concerned here with the agonist binding site of the nAChR. Early biochemical studies revealed several key features of this important region of the receptor. The nAChR has two binding sites which have been found to be localized primarily on the α subunits. Pioneering work by Karlin and colleagues established that a conserved disulfide bond in the α subunit (Cys 192–193, mouse muscle numbering) was near the binding site [13]. Photoaffinity labeling studies by Changeux and several radioligand binding studies [10,15] identified a large number of aromatic residues near the agonist binding site. Later work implicated residues in the γ and δ subunits that may contribute to acetylcholine (ACh) binding [16]. In addition, Unwin has produced a cryoelectron microscopy image of the receptor at 4.6 Å resolution. The cryoelectron microscopy reveals extracellular cavities in the two α subunits that lie above the membrane, about 50 Å away from the presumed gate of nAChR ion channel. It has been proposed that these cavities, which are not seen in the other subunits, represent the agonist binding sites [9]. However, even with these data, the location and nature of the agonist binding sites in the nAChR are highly debated.

1.1. Tethered agonist approach

We recently used the unnatural amino acid methodology to establish that a single residue in each mouse muscle α subunit, Trp 149, binds an ACh molecule through a cation–π interaction [17,18], defining a crucial component of the agonist binding site [12]. The primary tool was a comparison of affinities for a series of fluorinated Trp mutants to their predicted cation–π binding abilities, the latter determined by ab initio quantum mechanical calculations. To further establish Trp 149 as very near the agonist binding site, we incorporated the unnatural amino acid Tyr-O3Q (Fig. 2) at this position. The side chain of Tyr-O3Q contains a tethered quaternary ammonium group that was meant to mimic the analogous functional group in ACh. Incorporation of Tyr-O3Q at position α149 produced a constitutively active receptor, resulting in nicotinic receptor currents even in the absence of ACh.

The tethered agonist strategy has a distinguished history with the nAChR. In pioneering experiments, tethered agonists were introduced into the nAChR using chemical modification of Cys residues created by reduction of the Cys 192–193 disulfide bond (see Fig. 1), producing a constitutively active receptor [19,20]. Very recently, Cohen expanded on this methodology by introducing Cys residues using site-directed mutagenesis and then reacting the mutants with various MTS reagents [21]. We will discuss these results below.

The unnatural amino acid methodology offers an alternative and in some ways preferable strategy for introducing tethered agonists. Since the approach does not rely on cysteine modification, the tether can be incorporated at many different positions, including sites where the Cys mutant cannot produce functional receptors, and sites that are not accessible to external reagents, as might be expected at a potentially buried agonist binding site. This strategy also removes ambiguities in tether location that can arise if more than one cysteine is present in the molecule and allows a wider variation in functionality. In

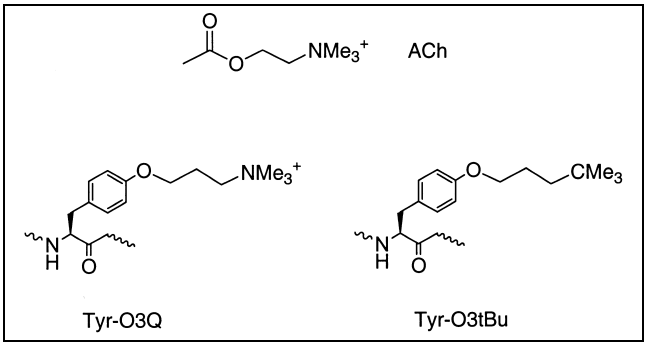

Fig. 2. Structures of ACh and two tethered agonist unnatural amino acids.

addition, agonist-like functionalities are introduced directly into the receptor, eliminating possibly deleterious side reactions associated with chemical modification strategies.

Here we expand upon our initial observations concerning a tethered agonist in several ways, and thereby establish the generality of the approach. We describe the novel synthetic approach to such unnatural amino acids; we show that varying the tether length produces a variation in tethered agonist efficiency; and we reveal two other sites – Tyr α93 and Trp γ55/δ57 – where the tethered agonist strategy is successful. We also discuss the results of incorporation of an isosteric but electronically neutral analog of Tyr-O3Q termed Tyr-O3tBu (Fig. 2), in which the quaternary ammonium is replaced by a tert-butyl group. With these new findings, a more advanced, but still speculative, model for the nAChR agonist binding site can be developed.

2. Results

2.1. Synthesis of Tyr-OnQ and Tyr-O3tBu

For use in the unnatural amino acid methodology, the synthetic target is the amino acid with the side chain in place, the amino group protected, and the carboxylate activated as a cyanomethyl ester [22], which is usually formed in the final step. However, this standard strategy was not successful when applied to a series of amino acids containing quaternary ammonium side chain groups. Instead, we find that the quaternary ammonium must be added at the final stage of the synthesis. A two step amination sequence is successful despite other potentially sensitive functionalities in the molecule. Fig. 3A summarizes the successful syntheses of Tyr-OnQ, with $n = 2$, 3, 4, and 5, followed by coupling with the dinucleotide dCA, which is a necessary step for unnatural amino acid mutagenesis [2]. We have also incorporated an isosteric analog of Tyr-O3Q, Tyr-O3tBu, to probe the role of charge in the function of the tethered agonists. The synthesis of Tyr-O3tBu was straightforward and is summarized in Fig. 3B.

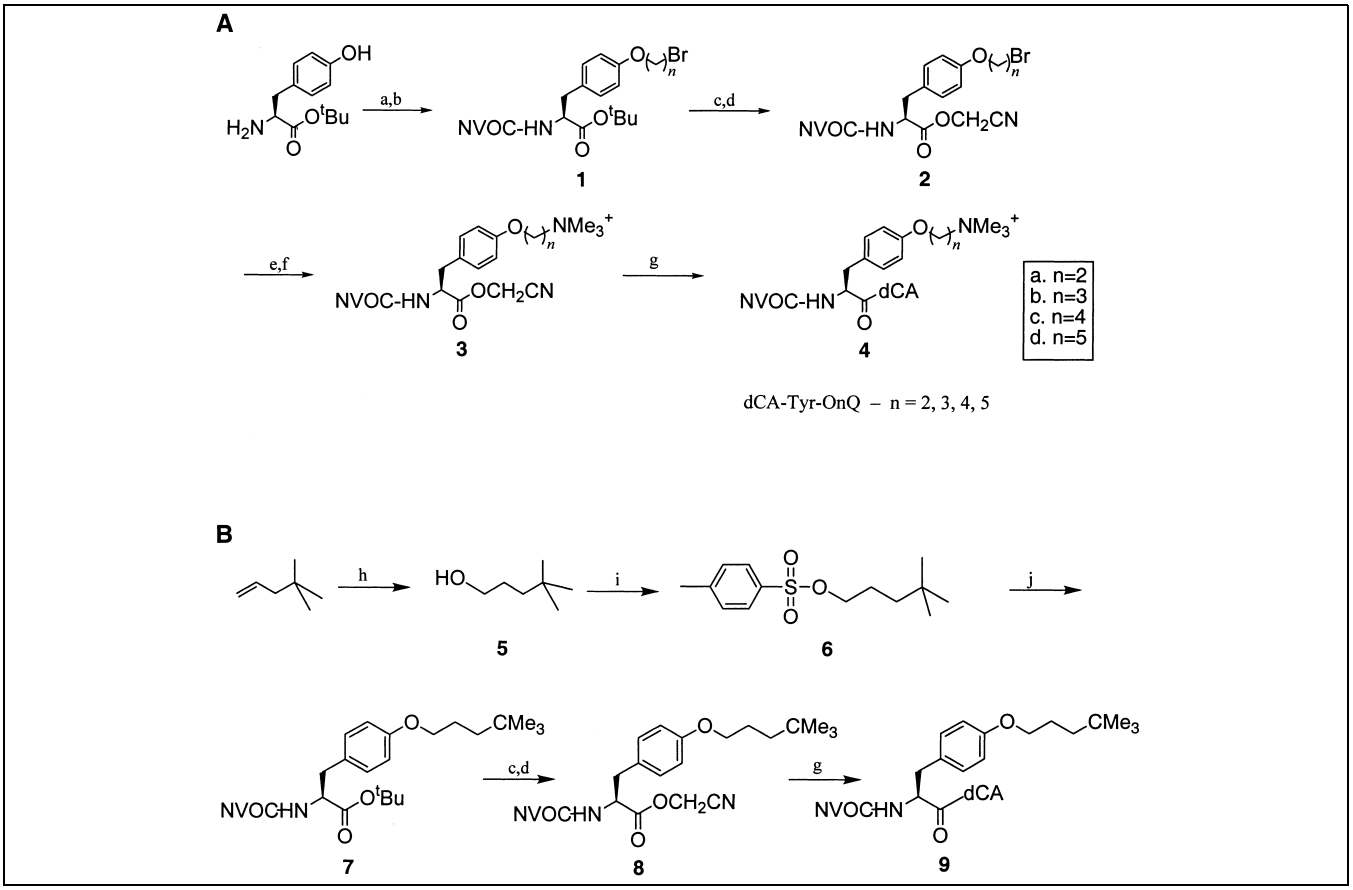

Fig. 3. A: Synthetic scheme for Tyr-OnQ. a: NVOC-Cl, Na_2CO_3, water/dioxane; b: Br-(CH_2)n-Br, Cs_2CO_3, DMF; c: TFA, CH_2Cl_2; d: $ClCH_2CN$, DMF/DIPEA; e: NaI, acetone; f: NMe_3, THF/toluene; g: dCA, DMF, tetrabutylammonium acetate. B: Synthetic scheme for Tyr-O3tBu. h: BH_3–THF, THF; then water, 3 M NaOH, 30% H_2O_2; i: *p*-toluene sulfonyl chloride, pyridine; j: NVOC-tyrosine *t*-butyl ester, K_2CO_3 acetone.

2.2. Incorporation of Tyr-OnQ into the nAChR

We attempted incorporation of the series of quaternary ammonium derivatives of tyrosine, Tyr-OnQ ($n = 2$, 3, 4 and 5), at several positions around the agonist binding sites of the nAChR, including: Trp α86, Tyr α93, Trp α149, Trp α184, Tyr α190, Cys α192, Cys α193, Pro α194, Tyr α198, Trp γ55/δ57 and Asp γ174/δ180. Thus, at least one site was probed on each of the five 'loops' (A–D, F) that have been proposed to define the ACh binding site (Fig. 1). Given the stoichiometry of the receptor, suppression in an α subunit incorporates two copies of the modified side chain, one associated with each of the two agonist binding sites of the receptor. For sites in non-α subunits, we always made two mutations – one in γ and one in the analogous site in δ – so that both agonist binding sites are comparably perturbed. Mutant proteins were expressed in *Xenopus* oocytes and whole-cell currents were measured using two-electrode voltage-clamp electrophysiology [2,23,24].

The hallmark of a successful experiment is the observation of large standing currents in *Xenopus* oocytes expressing the mutant channel in the absence of added ACh (Fig. 4, identified as a). The standing currents are reduced in the presence of the open-channel blocker 8-(*N,N*-diethylamino)octyl 3,4,5-trimethoxybenzoate (TMB-8). This establishes that the observed current is due to a nAChR, rather than a non-specific basal current in the oocyte. Note that TMB-8 blocks the channel by binding to the open state of the receptor in the pore region at a site that is quite far removed from the agonist binding site. As such, the mutations we are introducing should not impact the ability of TMB-8 to block constitutive current. In earlier studies involving Tyr-O3Q at position α149, we also used blockade by QX-314 and NMDG; dose-dependent antagonism by curare; desensitization of the standing current by longer application of ACh; and single channel measurements to associate the standing current with the nAChR [12].

In the present work, constitutively active receptors were observed at only three of the sites evaluated – Trp α149, Tyr α93 and Trp γ55/δ57. At the other sites the typical outcome was that no constitutive current that could be blocked by TMB-8 was seen. In some cases, very small, TMB-8 blockable constitutive currents were seen, but only when the expression level for the receptor was especially high, as indicated by large ACh-induced currents. We are reluctant to interpret such small currents. Concerning these other sites, it is, in general, risky to interpret 'failed' nonsense suppression experiments. It could well be that the unnatural amino acid failed to incorporate into the protein at the ribosome. Alternatively, 'failure' could mean that the unnatural amino acid was incorporated at the ribosome, but after incorporation the mutant protein failed in folding, or assembly, and/or transport to the cell membrane. Or perhaps receptors containing the tethered agonists were expressed on the surface of the oocyte, but

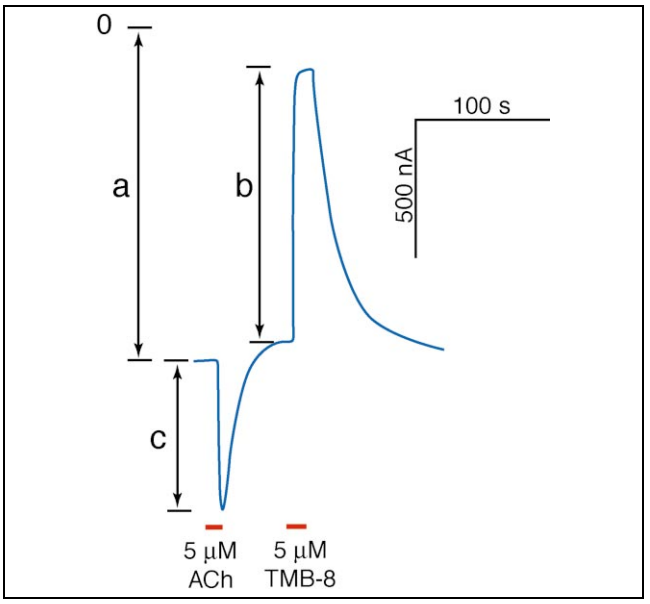

Fig. 4. Representative recording trace (blue) of voltage-clamp currents for an individual oocyte expressing mutant nAChR with Tyr-O3Q incorporated at α149. The red horizontal bars indicate bath application of ACh (5 μM) and TMB-8 (5 μM). a: Standing current due to constitutively active nAChR; b: standing current that is blocked by TMB-8; c: ACh-induced current.

the mutant protein is non-functional. Generally it is difficult to distinguish among these possibilities, and for the remainder of this work we will focus on the three sites that produced constitutively active receptors.

In addition to the channel blocker TMB-8, receptors were treated with the natural agonist ACh, and in all cases such treatment led to an increase in current. This establishes that a tethered quaternary ammonium group is a fairly weak agonist, a so-called partial agonist, meaning that full potency is never reached with the tether alone. Our earlier study [12] showed that, as expected, single channel conductance for the tethered system is identical to that of the native receptor, so it is the open probability that does not reach optimal values. Further supporting this view, standing currents are only observed when a mutation of Leu 262 (conventionally referred to as Leu 9′) to Ser is introduced into the channel (M2) region of the β subunit. Such a mutation is quite far removed from the agonist binding site and is well established to facilitate channel opening [12,25,26].

Fig. 4 defines the key parameters for evaluating tethered agonist experiments. It begins with a standing current that by convention is considered negative. For the particular oocyte shown, the value of the standing current (a) was −1200 nA. Application of 5 μM ACh causes a downward deflection, indicating an increase in current, and the magnitude of the ACh-induced current is c. After removal of ACh and reestablishment of a (slightly shifted) baseline, TMB-8 is added, and the drop in current is labeled b. Numerically, b is equal to the difference between the standing current and the current in the presence of

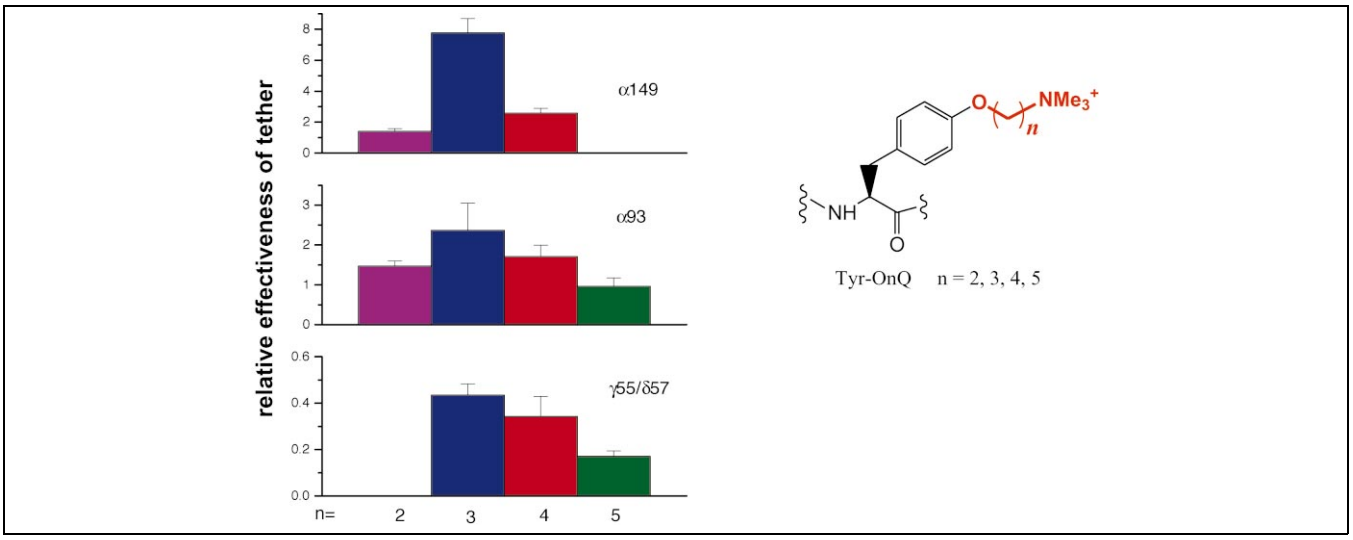

Fig. 5. Tethered agonist relative efficiencies (b/c per Fig. 4) for Tyr-OnQ as a function of *n* (the number of methylene groups in the side chain) at positions α149, α93, and γ55/δ57. Data shown are for an ACh concentration of 25 μM, although comparable results are seen with other concentrations.

TMB-8. As a gauge of the effectiveness of a given tether in opening the receptor, we use the ratio of the constitutive current that is blocked by TMB-8 to the ACh-induced current (Fig. 4, b/c). This measures the extent to which the tethered agonist opens the receptor relative to the presumed maximal response as seen with added ACh. Using this ratio minimizes complications due to variations in the expression level of the receptors in *Xenopus* oocytes. The larger the b/c ratio, the more effective the tethered agonist. We appreciate that this is an imperfect measure of the effectiveness of a tethered agonist, but we consider it to be a useful qualitative guideline. No quantitative significance is given to the ratios. Fig. 5 summarizes the results of incorporation of Tyr-OnQ into the nAChR at the three sites.

2.3. *Incorporation of an isosteric, neutral tether*

While Tyr-OnQ was designed to deliver a mimic of a key aspect of ACh – the quaternary ammonium group – it remained possible that the agonism seen in these experiments is due to some less specific effect, such as a simple steric disruption of the agonist binding site. To address this concern we prepared the isosteric compound of Tyr-O3Q, where the quaternary ammonium is substituted by a tert-butyl group (Fig. 2).

We incorporated Tyr-O3tBu at α149, α93 and γ55/δ57 sites. We found that incorporation of Tyr-O3tBu at α93 and γ55/δ57 does produce constitutively active receptors. In most cases Tyr-O3tBu is less effective than Tyr-O3Q, based on both the magnitude of the constitutive currents (data not shown) and the ratio of the TMB-8-blocked current to ACh-induced current (Fig. 6).

Upon attempted incorporation of Tyr-O3tBu at α149, the site at which Tyr-O3Q is most effective, no constitutive current is observed. In addition, only very small currents are observed upon application of ACh. This result could imply that receptors containing Tyr-O3tBu at α149 are not constitutively active and cannot be activated by ACh because the tert-butyl compound is obstructing the binding site. Alternatively, the results could signal that there are no receptors expressed on the surface of the oocytes. To discriminate between these two possibilities, further investigations were undertaken to determine whether nAChR are indeed expressed on the surface of the oocytes in the Tyr-O3tBu incorporation experiments. Using either binding studies on intact oocytes with [^{125}I]bungarotoxin (a tight-binding antagonist of the nAChR) or Western blot analyses of oocyte membranes (for experimental details, see Section 5), we found that indeed more nAChR are expressed on the surface of the oocyte when Tyr-O3Q is incorporated than Tyr-O3tBu. In fact, the apparent expression of Tyr-O3tBu is generally not above background levels seen in control suppression experiments.

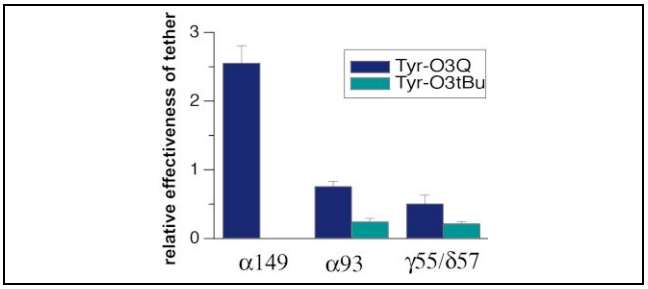

Fig. 6. Results of incorporation of Tyr-O3tBu compared with that of Tyr-O3Q at three sites of nAChR. The value plotted is the ratio of constitutive current that is blocked by TMB-8 (10 μM) to ACh (25 μM)-induced current, b/c in Fig. 4.

3. Discussion

The present study shows that the tethered agonist approach, as implemented by the in vivo nonsense suppression methodology, is a general tool that can provide valuable information about the agonist binding site of a neuroreceptor. Tethered agonists at three different sites give constitutively active receptors. Variations in tether length can discriminate among the different sites. In the particular case of the nAChR, we believe the results have significant implications for efforts to understand the structure of this complex protein.

In our preliminary report only Tyr-O3Q at position α149 was studied. We now find that tether length significantly influences the effectiveness of the agonist at this position. As shown in Fig. 5, Tyr-O3Q represents the most effective chain length. Both longer and shorter tethers are significantly less effective at inducing current – Tyr-O5Q produced no measurable constitutive current. We interpret this, in part, as a conformational effect. We concluded from our earlier studies that when ACh binds to the nAChR, the quaternary ammonium group makes van der Waals contact with the six-membered ring of Trp α149 through a cation–π interaction [12]. When Tyr-OnQ is incorporated at α149, its aromatic ring aligns with the five-membered ring of the wild type Trp. Note that an aromatic group is part of the Tyr-OnQ motif primarily for synthetic reasons. It is not anticipated that a cation–π interaction is involved between the tethered quaternary ammonium group and the aromatic of the side chain. The tether of Tyr-OnQ must curve around to position the quaternary ammonium above the site where the six-membered ring of the natural Trp would be. Modeling indicates that this is unlikely for a two-carbon tether, but is possible for tethers of length = 3. Perhaps the tethers of Tyr-OnQ are too long when $n = 4$ or 5, inflicting adverse steric interactions when positioning the quaternary ammonium appropriately. The strong preference for a three-carbon tether at position α149 suggests a fairly strict geometric requirement for achieving the maximum in constitutive activation.

We have also established that incorporation of tethered agonists at two other sites creates a constitutively active receptor. One of these sites is α93. Previous photoaffinity and site-directed mutagenesis studies have suggested that Tyr α93 is near the agonist binding site [6–8]. Our earlier evaluation of this residue using unnatural amino acid mutagenesis indicated that the OH of the Tyr forms an important hydrogen bond that affects agonist binding; however, ACh is not the acceptor of this hydrogen bond [23]. As shown in Fig. 5, Tyr-OnQ with $n = 2$–5 are comparably effective at α93, in contrast to the results for α149.

The other site where tethered agonists lead to a constitutively active receptor is γ55/δ57. All the tethers with long chains (≥3 carbons) are modestly effective at this site. This suggests that Trp γ55/δ57 must be fairly near the agonist binding site. However, it is likely to be further away than Trp α149 and Tyr α93, since the shortest tether is not effective. In fact, all tethers are less effective at Trp γ55/δ57 than at the other sites.

We note that the constitutive currents (Fig. 4, a) are consistently larger when Tyr-OnQ is incorporated at α149 than at α93 and γ55/δ57 (data not shown). This is not simply because the receptor expresses more efficiently with the tether at α149, since the ratio of TMB-8-blocked current to ACh-induced current shows the same trends. Apparently, Tyr-OnQ is able to position the quaternary ammonium more precisely and/or with less overall disruption of the receptor when it is delivered via α149 than α93 or γ55/δ57.

Interesting results are seen with Tyr-O3tBu, a tether that is isosteric to but lacks the positive charge of Tyr-O3Q. No constitutively active or ACh-induced currents are seen from efforts to incorporate Tyr-O3tBu at α149. We noted above the challenges of interpreting negative results from nonsense suppression experiments. However, at the Trp α149 site we know that: (a) nonsense suppression can be quite efficient if different unnatural amino acids are employed; (b) a sterically very similar residue (Tyr-O3Q) incorporates efficiently; (c) the desired residue, Tyr-O3tBu, does incorporate at other sites (see below) and therefore is compatible with the ribosomal machinery. Although not completely conclusive, efforts to determine whether the receptor containing Tyr-O3tBu was successfully synthesized, assembled, and transported to the surface suggest that it was not. For the reasons enumerated above, we consider it unlikely that this represents a failure of the nonsense suppression methodology. We think it more likely that a receptor with Tyr-O3tBu incorporated at position α149 does not fold or does not assemble properly, and therefore no receptor appears on the surface. Thus, the immediate vicinity of the agonist binding site – the region very near Trp α149 – is quite sensitive, accepting a very close analog of its natural ligand, Tyr-O3Q, but nothing else.

At α93 and γ55/δ57, Tyr-O3tBu is incorporated and gives measurable constitutive currents, but less than the cationic analog. While direct contact between ACh and Trp α149 is well established, such is not the case for Tyr α93 nor Trp γ55/δ57. We propose that these 'secondary' sites are less intimately involved in defining the agonist binding site, but are better described as nearby. Incorporating the tether at these sites disrupts the binding region, partly through a simple steric effect, since Tyr-O3tBu works. However, a tethered quaternary ammonium is more effective, suggesting these remote sites do sense some of the binding interactions associated with the quaternary ammonium on ACh.

It is important to appreciate that gating an ion channel is a complex process. An agonist must bind to the receptor and initiate opening of the ion channel. This is made even more complicated in the nAChR, where the ion channel

and its gate are structurally remote from the agonist binding site [9,27]. In such a system, it is envisioned that binding of agonist induces a conformational change that shifts a pre-existing equilibrium between closed and open states of the channel toward the open state. It is easy to imagine that the structural perturbation of introducing Tyr-OnQ or Tyr-O3tBu at one of the secondary sites could disrupt the structure of the protein in the vicinity of the agonist binding site in the direction of the conformational change associated with opening. Note that in all cases the tethered agonist is a weak agonist, indicating that the full effect on the open/closed equilibrium elicited by ACh is never achieved with a tethered agonist. The tethered agonist essentially pushes the receptor along the path toward opening, or, stated differently, perturbs the gating equilibrium, but less effectively than the true agonist. Precisely at the agonist binding site, α149, the structural requirements are more strict, and an optimal tether produces a large effect.

Very recently, Sullivan and Cohen described tethered agonist studies in which potential tethered agonists were incorporated by reacting Cys residues introduced by site-directed mutagenesis with various MTS reagents [21]. At α149 the Cys mutation made the receptor unresponsive to ACh, which is not surprising given the crucial role of Trp α149 in agonist binding [12]. At α93, Cys modification resulted in irreversible inhibition, while at γ55 there was no effect for the Cys mutants after treatment with MTS reagents. Interestingly, though, reaction of the α198 Tyr/Cys mutant with MTSET produced a constitutively active receptor. This effect was seen without the additional Leu9′Ser mutation required in the present studies, which could indicate quite efficient activation. The effect at α198 was quite sensitive to the length and orientation of the tethered group, in that lengthening or shortening the tether by one methylene group negated the tethered agonist effect. The successful tether introduced by MTS modification ($C_\alpha CH_2SSCH_2CH_2NMe_3^+$) is much shorter than those investigated here, and so our failure to see constitutive activation with Tyr-OnQ at α198 is not surprising.

3.1. *An emerging model of the agonist binding site of the nAChR*

Efforts to develop a detailed picture of the agonist binding site of the nAChR continue in many labs. Efforts to date are schematized in Fig. 1. The binding site involves several key residues located on several discontinuous 'loops'. A large number of aromatic residues are associated with the agonist binding site, along with perhaps one anionic residue. One residue in particular, Trp α149, has been shown to contact the agonist in the binding site [12].

Another relevant observation is the high resolution crystal structure of acetylcholine esterase (AChE) [28], the only natural ACh binding site for which such a structure is available. As was anticipated [29], a cation–π interaction is crucial for binding ACh. In fact, the esterase uses a tryptophan, Trp 84, to bind the quaternary ammonium group of ACh. In addition, the esterase features a 20 Å 'aromatic gorge' that leads from the surface of the enzyme to the active site and Trp 84. The gorge is lined with over a dozen conserved aromatic residues that presumably guide the ACh to the active site using cation–π interactions and other effects. This structure was revealed at about the same time that many workers were identifying the large number of aromatic residues associated with the agonist binding site of the nAChR. The possibility that a comparable aromatic gorge would exist in the nAChR was immediately apparent. Recently, Unwin has interpreted electron densities in the vicinity of the agonist binding site as consistent with such a gorge, but the images are not yet of sufficient resolution to be decisive [9].

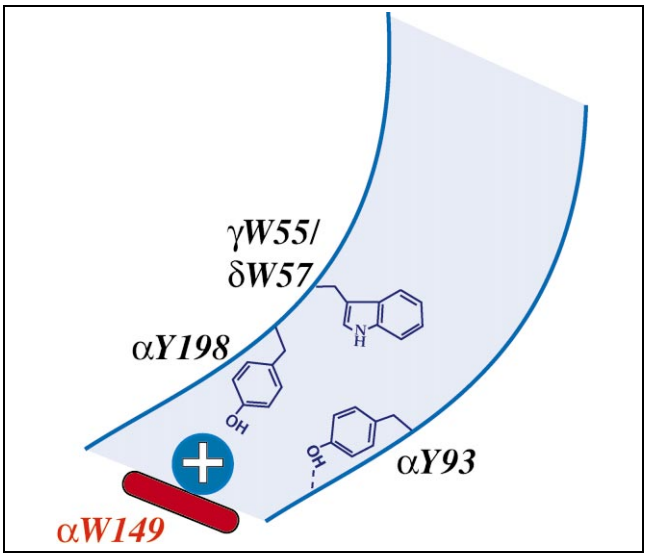

Fig. 7. The evolving view of the nAChR agonist binding site. Shown is a highly schematic view of an 'aromatic gorge' analogous to that proposed for ACh esterase. Trp α149 lies at the bottom of the gorge and binds the quaternary ammonium group of ACh, playing the role of Trp 84 in the AChE. Tyr α198 is near the bottom of the gorge, while Tyr α93 lies slightly up the gorge, and its OH forms an important hydrogen bond. Trp γ55/δ57 lies further up the gorge.

If an aromatic gorge analogous to the one found in the AChE exists in the nAChR, then the results presented here put certain constraints on the model, as summarized in Fig. 7. Certainly, the bottom of the gorge and the final resting place of ACh are defined by Trp α149, playing the role ascribed to Trp 84 in the esterase. Note that of all the residues discussed as contributing to or being near the agonist binding site (Fig. 1), evidence for direct interaction with ACh exists only for Trp α149. The relatively strict structural requirement at Trp α149 proposed here is consistent with the absence of ACh response seen for the Cys mutant at this site [21]. We propose that Tyr α93 is near the bottom of the gorge, as evidenced by the fact that the shortest tether elicits a response at this site. The OH of Tyr α93 is involved in a key hydrogen bond in the binding site, and we suggest this is a hydrogen bond to the protein

backbone [23]. Given that tethered agonists at γ55/δ57 had a weaker ability to open the channel and that the two-carbon tether is ineffectual, we position γ55/δ57 further up the gorge. An ongoing debate in the nAChR literature is whether the agonist binding site is best thought of as being buried within the α subunits or whether it is at the subunit interfaces, α/δ and α/γ. Our results clearly support a role for the γ/δ subunits. However the α/δ and α/γ subunit interfaces might be contributing to the gorge leading to the agonist binding site, rather than actually structuring the binding site. Finally, we include Tyr α198 as very near the agonist binding site, based on the MTS studies of Cohen. Of course, the model presented in Fig. 7 is highly speculative at this point, and we look forward to further studies – both structural and mechanistic – to refine it.

4. Significance

In summary, we have shown that the tethered agonist approach via unnatural amino acid mutagenesis is a general tool for probing structure in the nAChR. We fully expect it will be useful in other integral membrane proteins. We have now positioned three residues – Trp α149, Tyr α93 and Trp γ55/δ57 – very near the agonist binding site and each with a distinct role. We anticipate that further application of this methodology will provide additional, useful insights.

5. Materials and methods

5.1. Chemicals

Reagents were purchased from Aldrich, Sigma, or other commercial sources. TMB-8 was purchased from RBI (Natick, MA, USA). Anhydrous THF was distilled from sodium benzophenone; anhydrous methylene chloride, toluene and acetonitrile were distilled from CaH_2; anhydrous acetone was distilled from $CaSO_4$; anhydrous DMF was obtained from Fluka. Flash chromatography was on 230–400 mesh silica gel with the solvent indicated. All NMR shifts are reported as δ ppm downfield from TMS. ^{1}H NMR spectra were recorded at 300 MHz in $CDCl_3$ using a GE QE-300 spectrometer. FAB-MS determinations were performed at University of Nebraska-Lincoln. Electrospray (ESI) ionization, quadrupole mass spectrometry was performed at the Caltech Protein/Peptide Micro Analytical Laboratory. High performance liquid chromatography (HPLC) separations were performed on a Waters dual 510 pump liquid chromatography system equipped with a Waters 490E variable wavelength UV detector. Semi-preparative samples were separated using a Whatman Magnum 9 column (9.4×500 mm, Partisil 10, ODS-3). Nitroveratryloxycarbonyl chloride (NVOC-Cl) and NVOC-tyrosine *t*-butyl ester were prepared as described earlier [23].

5.2. Synthesis of Tyr-OnQ

5.2.1. NVOC-O-(2-bromoethyl) tyrosine t-butyl ester (1a)

To a mixture of 0.690 ml (8 mmol, 16 equivalents) of 1,2-dibromoethane and 330 mg (1 mmol, two equivalents) of Cs_2CO_3 in 15 ml of anhydrous DMF was added a solution of 238 mg (0.5 mmol) of NVOC-tyrosine *t*-butyl ester in 10 ml of DMF slowly over 10 h using a syringe pump. After stirring overnight, the reaction mixture was quenched by adding 30 ml of water and extracted by 3×30 ml of ethyl acetate. The combined organic layers were washed with water once, dried (over Na_2SO_4), rotary-evaporated, and chromatographed (30:70 ethyl acetate:petroleum ether), providing 61 mg (21%) of product. ^{1}H NMR ($CDCl_3$): δ 7.69 (s, 1H), 7.05 (d, 2H), 6.95 (s, 1H), 6.81 (d, 2H), 5.54 and 5.46 (AB, 1H), 5.32 (d, 1H), 4.48 (m, 1H), 4.24 (t, 2H), 3.93 (s, 6H), 3.61 (t, 2H), 3.03 (m, 2H), 1.41 (s, 9H).

5.2.2. NVOC-O-(3-bromopropyl) tyrosine t-butyl ester (1b)

This compound was prepared by the procedure described above. Yield 57%. ^{1}H NMR ($CDCl_3$): δ 7.68 (s, 1H), 7.07 (d, 2H), 6.96 (s, 1H), 6.84 (d, 2H), 5.54 and 5.45 (AB, J = 15.2 Hz, 1H), 5.33 (d, 1H), 4.50 (m, 1H), 4.07 (m, 2H), 3.95 (s, 6H), 3.60 (t, 2H), 3.05 (m, 2H), 2.31 (m, 2H), 1.42 (s, 9H).

5.2.3. NVOC-O-(4-bromobutyl) tyrosine t-butyl ester (1c)

This compound was prepared by the procedure described above. Yield 67%. ^{1}H NMR ($CDCl_3$): δ 7.68 (s, 1H), 7.06 (d, 2H), 6.94 (s, 1H), 6.77 (d, 2H), 5.53 and 5.45 (AB, 1H), 5.35 (d, 1H), 4.46 (m, 1H), 3.94 (m, 2H), 3.92 (s, 6H), 3.46 (t, 2H), 3.01 (m, 2H), 2.02 (m, 2H), 1.90 (m, 2H), 1.40 (s, 9H).

5.2.4. NVOC-O-(5-bromopentyl) tyrosine t-butyl ester (1d)

This compound was prepared by the procedure described above. Yield 58%. ^{1}H NMR ($CDCl_3$): δ 7.52 (s, 1H), 6.94 (d, 2H), 6.82 (s, 1H), 6.65 (d, 2H), 5.61 (d, 1H), 5.32 (m, 2H), 4.35 (m, 1H), 3.96 (m, 2H), 3.77 (s, 6H), 3.28 (t, 2H), 2.91 (m, 2H), 1.77 (m, 2H), 1.65 (m, 2H), 1.40 (m, 2H), 1.27 (s, 9H).

5.2.5. NVOC-O-(4-bromobutyl) tyrosine cyanomethyl ester (2c)

To a solution of 290 mg (0.48 mmol) of azeotropically dried (with toluene) NVOC-*O*-(1-(4-bromobutyl)) tyrosine *t*-butyl ester in 1.7 ml of dry CH_2Cl_2 was slowly added 2.8 ml of TFA (37.2 mmol, 77.5 equivalents). The mixture was stirred under argon at room temperature for 2 h. TFA was removed by passing argon through the reaction solution. The residue was rotary-evaporated with toluene twice (2×10 ml), dried under vacuum and then used directly in the next step. To this crude product was added 5 ml of anhydrous DMF, 0.67 ml (10.5 mmol, 21.8 equivalents) of chloroacetonitrile and 96 μl of diisopropylethylamine. The mixture was stirred at room temperature overnight. After about 14 h the reaction was quenched by adding 10 ml of 0.1 M KH_2PO_4 and 10 ml of water and then extracted with 2×50 ml of ethyl acetate. The combined organic layers were washed with water, dried (over Na_2SO_4) and rotary-evaporated. Flash chromatography (1:3 to 2:3 ethyl acetate:petroleum ether) gave 210 mg (74%)

of product. ^{1}H NMR ($CDCl_3$): δ 7.66 (s, 1H), 7.03 (d, 2H), 6.89 (s, 1H), 6.80 (d, 2H), 5.51 and 5.41 (AB, 1H), 5.38 (d, 1H), 4.72 (m, 3H), 3.94 (m, 2H), 3.91 (s, 6H), 3.58 (t, 1H), 3.45 (t, 1H), 3.07 (m, 2H), 2.01 (m, 2H), 1.92 (m, 2H).

5.2.6. NVOC-O-(2-bromoethyl) tyrosine cyanomethyl ester (2a)

This compound was prepared by the procedure described above. Yield 58%. ^{1}H NMR ($CDCl_3$): δ 7.70 (s, 1H), 7.07 (d, 2H), 6.92 (s, 1H), 6.87 (d, 2H), 5.56 and 5.45 (AB, 1H), 5.29 (d, 1H), 4.76 (m, 3H), 4.27 (t, 2H), 3.95 (s, 6H), 3.63 (t, 2H), 3.10 (m, 2H).

5.2.7. NVOC-O-(3-bromopropyl) tyrosine cyanomethyl ester (2b)

This compound was prepared by the procedure described above. Yield 93%. ^{1}H NMR ($CDCl_3$): δ 7.66 (s, 1H), 7.04 (d, 2H), 6.90 (s, 1H), 6.83 (d, 2H), 5.54 and 5.45 (AB, J = 15.2 Hz, 1H), 5.46 (b, 1H), 4.74 (m, 3H), 4.06 (m, 2H), 3.93 (s, 6H), 3.57 (t, 2H), 3.08 (m, 2H), 2.28 (m, 2H).

5.2.8. NVOC-O-(5-bromopentyl) tyrosine cyanomethyl ester (2d)

This compound was prepared by the procedure described above. Yield 69%. ^{1}H NMR ($CDCl_3$): δ 7.61 (s, 1H), 7.01 (d, 2H), 6.86 (s, 1H), 6.77 (d, 2H), 5.53 (d, 1H), 5.46 and 5.37 (AB, 1H), 4.71 (m, 3H), 3.89 (m, 2H), 3.87 (s, 6H), 3.51 (t, 1H), 3.38 (t, 1H), 3.05 (m, 2H), 1.87 (m, 2H), 1.75 (m, 2H), 1.56 (m, 2H).

5.2.9. NVOC-O-(4-(N,N,N-trimethylammonium)butyl) tyrosine cyanomethyl ester (NVOC-Tyr-O4Q) (3c)

200 mg (0.337 mmol) of NVOC-*O*-(1-(4-bromobutyl)) tyrosine cyanomethyl ester was mixed with 650 mg (4.333 mmol, 12.5 equivalents) of sodium iodide in 10 ml of acetone at room temperature. The reaction was kept stirring in the dark overnight. Acetone was then rotary-evaporated off, and the solid was partitioned between water and methylene chloride (30 ml each). The aqueous layer was extracted with methylene chloride once. Organic layers were combined, washed with water once, dried (over Na_2SO_4), and rotary-evaporated to give 200 mg (93%) of yellowish solid NVOC-*O*-(1-(4-iodobutyl)) tyrosine cyanomethyl ester. Half of this product was carried on to make NVOC-*O*-(1-(4-(*N,N,N*-trimethylammonium)-butyl)) tyrosine cyanomethyl ester. The solution of the iodide in 7 ml of dry toluene and 12 ml of dry THF was cooled to 0°C in an ice/NaCl bath. Then trimethylamine was passed through the solution via a metal needle for about 5 min. The solution was allowed to warm up to room temperature and stirred in the dark for 32 h. Precipitate formed on the inner wall of the flask. Argon was passed through to get rid of the amine, which was trapped by 6 N HCl. When most of the amine was removed (indicated as neutral by wet pH paper), the solution was decanted and the solid was rinsed with ethyl acetate three times and dried under vacuum. Yield 70 mg (68%). ^{1}H NMR ($CDCl_3$): δ 7.74 (s, 1H), 7.23 (d, 2H), 7.13 (s, 1H), 6.91 (d, 2H), 6.46 (d, 1H), 5.46 and 5.39 (AB, 1H), 4.85 (s, 2H), 4.52 (m, 1H), 4.05 (t, 2H), 3.96 (s, 3H), 3.93 (s, 3H), 3.39 (m, 2H), 3.10 (s, 9H), 3.00 (m, 2H), 1.98 (m, 2H), 1.85 (m, 2H).

5.2.10. NVOC-O-(2-(N,N,N-trimethylammonium)ethyl) tyrosine cyanomethyl ester (NVOC-Tyr-O2Q) (3a)

This compound was prepared by the procedure described above. Yield 85%. ^{1}H NMR ($CDCl_3$): δ 7.73 (s, 1H), 7.26 (d, 2H), 7.11 (s, 1H), 6.94 (d, 2H), 6.41 (d, 1H), 5.44 and 5.37 (AB, 1H), 4.83 (s, 2H), 4.55 (m, 1H), 4.41 (m, 2H), 3.95 (s, 3H), 3.92 (s, 3H), 3.74 (m, 2H), 3.20 (s, 9H), 3.01 (m, 2H).

5.2.11. NVOC-O-(3-(N,N,N-trimethylammonium)propyl) tyrosine cyanomethyl ester (NVOC-Tyr-O3Q) (3b)

This compound was prepared by the procedure described above. Yield 85%. ^{1}H NMR ($CDCl_3$): δ 7.72 (s, 1H), 7.22 (d, 2H), 7.09 (s, 1H), 6.88 (d, 2H), 6.36 (b, 1H), 5.54 and 5.45 (AB, J = 15.2, 1H), 4.82 (s, 2H), 4.50 (m, 1H), 4.07 (m, 2H), 3.95 (s, 3H), 3.90 (s, 3H), 3.47 (t, 2H), 3.08 (m, 9H), 2.98 (m, 2H), 2.00–2.10 (shoulder, 2H).

5.2.12. NVOC-O-(5-(N,N,N-trimethylammonium)pentyl) tyrosine cyanomethyl ester (NVOC-Tyr-O5Q) (3d)

This compound was prepared by the procedure described above. Yield 74%. ^{1}H NMR ($CDCl_3$): δ 7.72 (s, 1H), 7.20 (d, 2H), 7.11 (s, 1H), 6.87 (d, 2H), 6.47 (d, 1H), 5.44 and 5.37 (AB, 1H), 4.83 (s, 2H), 4.51 (m, 1H), 4.00 (t, 2H), 3.92 (s, 3H), 3.90 (s, 3H), 3.31 (m, 2H), 3.13 (m, 2H), 3.08 (s, 9H), 1.98 (m, 2H), 1.83 (m, 2H), 1.53 (m, 2H).

5.3. Synthesis of Tyr-O3tBu

5.3.1. 4,4′-Dimethylpentanol (5)

To a solution of 2 ml (13.9 mmol) 4,4′dimethylpentene in 6 ml of anhydrous THF at −78°C was added 13.9 ml of a 1 M BH_3–THF complex solution over 10 min via a syringe pump. The reaction mixture was stirred at −78°C for 45 min, then allowed to warm to room temperature and stirred for an additional 45 min. The reaction mixture was cooled to 0°C and 1.39 ml H_2O, 1.86 ml 3 M NaOH, and 2.5 ml 30% H_2O_2 were added. The solution was stirred for 72 h, extracted with 25 ml ether, and washed with 2×5 ml ice-cold H_2O followed by 2×5 ml saturated NaCl salt solution. The organic layer was dried over $MgSO_4$ and rotary-evaporated to give 1.124 g (70% yield). ^{1}H NMR ($CDCl_3$): δ 7.31 (s, 1H), 3.77 (t, 2H), 1.58 (m, 2H), 1.27 (m, 2H), 0.93 (s, 9H).

5.3.2. 4,4′-Dimethyl pentyl tosylate (6)

To a solution of 957 mg (8.25 mmol) 4,4′-dimethylpentanol in 8 ml anhydrous pyridine at 0°C was added 3.15 g (16.5 mmol) *p*-toluene sulfonyl chloride. The reaction mixture was slowly warmed to room temperature and stirred for 36 h. The reaction mixture was poured over 3 g ice and extracted with 6×5 ml dichloromethane, 6×5 ml ether, and 6×5 ml chloroform. The organic layers were washed using 2×1 ml 6 N HCl, 2×1 ml saturated $NaHCO_3$ salt solution, and 2×1 ml saturated NaCl salt solution. The organic layers were combined, dried over $MgSO_4$, and concentrated under vacuum to give 1.106 g (49.6% yield). The product was purified by flash chromatography (30:70 ethyl acetate:petroleum ether) to give 174.2 mg. ^{1}H NMR

($CDCl_3$): δ 7.75 (d, 2H), 7.31 (d, 2H), 3.98 (t, 2H), 2.39 (s, 3H), 1.53 (m, 2H), 1.12 (m, 2H), 0.78 (s, 9H).

5.3.3. NVOC-O-(4,4′-dimethyl pentyl) tyrosine t-butyl ester (7)

To a mixture of 486 mg (3.52 mmol) K_2CO_3 and 115.6 mg (0.243 mmol) NVOC-tyrosine *t*-butyl ester in 1 ml of anhydrous acetone was added a solution of 65.6 mg (0.243 mmol) 4,4′-dimethylpentyl tosylate in 1.5 ml anhydrous acetone. Another 2.4 ml anhydrous acetone was added to reaction mixture via a syringe to bring the total volume of solvent to 4.9 ml. The reaction mixture was refluxed for 60 h, quenched with 15 ml water, and extracted with 4×10 ml ether. The organic layers were combined, dried under $MgSO_4$, and concentrated by rotary evaporation. The product was purified by flash chromatography (20:80 ethyl acetate:petroleum ether) to give approximately 60 mg (~40% yield). ^{1}H NMR ($CDCl_3$): δ 7.68 (s, 1H), 7.03 (d, 2H), 6.95 (s, 1H), 6.80 (d, 2H), 5.48 (m, 2H), 5.28 (d, 1H), 4.70 (m, 1H), 3.92 (m, 6H), 3.85 (m, 2H), 3.04 (t, 2H), 1.73 (m, 2H), 1.40 (s, 9H), 1.26 (m, 2H), 0.89 (s, 9H).

5.3.4. NVOC-O-(4,4′-dimethyl pentyl) tyrosine cyanomethyl ester (8)

To a solution of 60 mg of the above product in 2 ml dichloromethane was added 1 ml TFA and stirred for 1 h. The TFA was removed under vacuum. The product was purified by flash chromatography using CH_2Cl_2 followed by CH_2Cl_2 with 1% acetic acid. The product was concentrated by rotary evaporation and then dissolved in 3 ml DMF. To the solution 0.6 ml chloroacetonitrile (9.5 mmol) and 16 µl triethylamine were added, and the reaction mixture was allowed to stir for 2 days. The reaction was quenched with 10 ml 0.1 M potassium phosphate solution and 20 ml H_2O. The product was extracted with 3×30 ml CH_2Cl_2, dried over $NaSO_4$, and concentrated under vacuum. The product was purified by flash chromatography (20:80 ethyl acetate:petroleum ether) to give approximately 20 mg (~65% yield). ^{1}H NMR ($CDCl_3$): δ 7.68 (s, 1H), 7.02 (d, 2H), 6.90 (s, 1H), 6.84 (d, 2H), 5.46 (m, 2H), 5.28 (d, 1H), 4.77 (s, 2H), 4.70 (m, 1H), 3.93 (m, 6H), 3.86 (m, 2H), 3.07 (d, 2H), 1.73 (m, 2H), 1.27 (m, 2H), 0.90 (s, 9H).

5.4. General procedure for coupling of amino acid to dCA

This method is essentially as described [22,23]. The N-protected amino acid (~30 µmol, three equivalents) was mixed with tetra-*n*-butyl-ammonium salt of the dCA dinucleotide (~10 µmol, one equivalent) in 400 µl of dry DMF. The reaction mixtures are kept stirring for 1–2 h. The crude product was separated using reverse-phase semi-preparative HPLC with a gradient from 25 mM ammonium acetate (pH 4.5) to CH_3CN. The desired fractions containing the aminoacyl dinucleotide were combined, frozen, and lyophilized. The lyophilized solid was redissolved in 10 mM aqueous acetic acid/acetonitrile and lyophilized a second time to remove salts. The products were quantified by UV/Vis spectra and characterized by mass spectrometry.

5.4.1. dCA-NVOC-O-(1-(2-(N,N,N-trimethylammonium)ethyl)) tyrosine (dCA-Tyr-O2Q) (4a)

Prepared as above: FAB-MS: [M^+], calculated for $C_{43}H_{56}N_{11}O_{21}P_2$: 1124.3128; found: 1124.2.

5.4.2. dCA-NVOC-O-(1-(3-(N,N,N-trimethylammonium)-propyl)) tyrosine (dCA-Tyr-O3Q) (4b)

Prepared as above: FAB-MS: [M^+], calculated for $C_{44}H_{57}N_{11}O_{21}P_2$: 1137.5; found: 1137.

5.4.3. dCA-NVOC-O-(1-(4-(N,N,N-trimethylammonium)butyl)) tyrosine (dCA-Tyr-O4Q) (4c)

Prepared as above: FAB-MS: [M^+], calculated for $C_{45}H_{60}N_{11}O_{21}P_2$: 1152.3440; found: 1152.3.

5.4.4. dCA-NVOC-O-(1-(5-(N,N,N-trimethylammonium)pentyl)) tyrosine (dCA-Tyr-O5Q) (4d)

Prepared as above: FAB-MS: [M^+], calculated for $C_{46}H_{62}N_{11}O_{21}P_2$: 1166.3596; found: 1166.4.

5.4.5. dCA-NVOC-O-(4,4′-dimethyl pentyl) tyrosine (dCA-Tyr-O3tBu) (9)

Prepared as above except that a catalytic amount of tetrabutylammonium acetate was added to the reaction mixture. ESI-MS; calculated for $C_{45}H_{57}N_{10}O_{21}P_2$: 1135.3175; found [M-H]$^-$ 1135.72.

5.5. Unnatural amino acid mutagenesis and oocyte injection

The site-directed mutagenesis of the nAChR TAG mutants, gene construction and synthesis of suppressor tRNA and ligation of aminoacyl-dCA to tRNA have been described previously [1–3,30]. Plasmid DNAs were linearized with *Not*I, and mRNA was transcribed using the Ambion (Austin, TX, USA) T7 mMESSAGE mMACHINE kit.

Oocytes were removed from *Xenopus laevis* as described [31] and maintained at 18°C, in ND96 solution (96 mM NaCl/2 mM KCl/1.8 mM $CaCl_2$/1 mM $MgCl_2$/5 mM HEPES/2.5 mM sodium pyruvate/0.5 mM theophyline/10 g/ml gentamicin, pH 7.5, with NaOH). Before microinjection, the NVOC-aminoacyl-tRNA was deprotected by irradiating the sample for 5 min with a 1000 W xenon arc lamp (Oriel) operating at 600 W equipped with WG-335 and UG-11 filters (Schott, Duryea, PA, USA). Each oocyte was injected with a 1:1 mixture of deprotected aminoacyl-tRNA (25–50 ng) and mRNA (12.5–18 ng of total at a concentration ratio of 20:1:1:1 for α:β:γ:δ subunits) in a volume of 50 nl. Since the presence of constitutively active channels would be expected to compromise the health of the oocytes through a large leak current, 2–5 µM TMB-8 was added to the incubation solution to block any leak current that might occur through the nAChR.

5.6. Electrophysiology

Electrophysiological recordings were carried out 24–48 h after injection. Whole-cell currents from oocytes were measured using

a Geneclamp 500 amplifier and pCLAMP software (Axon Instruments, Foster City, CA, USA) in the two-electrode voltage-clamp configuration. Microelectrodes were filled with 3 M KCl and had resistances ranging from 0.5 to 1.5 MΩ. Oocytes were continuously perfused with a nominally calcium-free bath solution consisting of 96 mM NaCl, 2 mM KCl, 1 mM $MgCl_2$, and 5 mM HEPES (pH 7.5). Microscopic ACh-induced and TMB-8-blocked currents were recorded in response to bath application of ACh (25 μM) and TMB-8 (5 μM or 10 μM) at a holding potential of −80 mV. All numerical and plotted data are from measurements obtained from 4–8 oocytes and are reported as mean ± S.E.M.

5.7. Bungarotoxin binding and Western blot analysis

[^{125}I]Bungarotoxin binding experiments were performed as described [32]. Oocytes were incubated in 400 μl of calcium-free ND96 (see Section 5.6) containing 10 mg/ml bovine serum albumin (Sigma) for 10 min and then [^{125}I]bungarotoxin (Amersham) was added to a final concentration of 1 nM. After incubation for 2 h, the oocytes were washed extensively and then counted in a Beckman LS5000 γ-counter.

Western blot analyses were carried out as described [33]. A hemagglutinin (HA) epitope was subcloned into the intracellular loop between the third and fourth transmembrane domains of the α subunit. The vitelline/plasma membranes were manually stripped from oocytes expressing nAChR [34]. Alternatively, the oocytes were treated with sulfo-NHS-LC-biotin (Pierce) and then homogenized. After removing the yolks of the oocytes by a centrifuge, the remaining supernatant was incubated with streptavidin-agarose beads (Sigma). The protein was then eluted from the beads by adding sodium dodecyl sulfate (SDS) buffer. In either case, the samples were analyzed by SDS–PAGE, followed by immunoblotting with the anti-HA antibody (BabCO, cat. # MMS-101R), and visualized using an ECL detection kit (Amersham).

Acknowledgements

ESI ionization, quadrupole mass spectrometry was carried out at the Caltech Protein Microanalytical Laboratory under the direction of Gary M. Hathaway. This work was supported by the NIH (NS 34407 and NS 11756).

References

[1] M.W. Nowak et al., Nicotinic receptor binding site probed with unnatural amino-acid incorporation in intact cells, Science 268 (1995) 439–442.
[2] M.W. Nowak, J.P. Gallivan, S.K. Silverman, C.G. Labarca, D.A. Dougherty, H.A. Lester, In vivo incorporation of unnatural amino acids into ion channels in a *Xenopus* oocyte expression system, Methods Enzymol. 293 (1998) 504–529.
[3] C.J. Noren, S.J. Anthony-Cahill, M.C. Griffith, P.G. Schultz, A general method for site-specific incorporation of unnatural amino acids into proteins, Science 244 (1989) 182–188.
[4] J.D. Bain, C.G. Glabe, T.A. Dix, A.R. Chamberlin, Biosynthetic site-specific incorporation of a non-natural amino acid into a polypeptide, J. Am. Chem. Soc. 111 (1989) 8013–8014.
[5] M. Lodder, S. Golvine, S.M. Hecht, Chemical deprotection strategy for the elaboration of misacylated transfer RNA's, J. Org. Chem. 62 (1997) 778–779.
[6] H.A. Lester, The permeation pathway of neurotransmitter-gated ion channels, Annu. Rev. Biophys. Biomol. Struct. 21 (1992) 267–292.
[7] A. Karlin, M.H. Akabas, Toward a structural basis for the function of nicotinic acetylcholine receptors and their cousins, Neuron 15 (1995) 1231–1244.
[8] A. Devillers-Thiéry, J.L. Galzi, J.L. Eiselé, S. Bertrand, D. Bertrand, J.P. Changeux, Functional architecture of the nicotinic acetylcholine receptor: a prototype of ligand-gated ion channels, J. Membr. Biol. 136 (1993) 97–112.
[9] A. Miyazawa, Y. Fujiyoshi, M. Stowell, N. Unwin, Nicotinic acetylcholine receptor at 4.6 Å resolution: transverse tunnels in the channel wall, J. Mol. Biol. 288 (1999) 765–786.
[10] F. Hucho, V.I. Tsetlin, J. Machold, The emerging three-dimensional structure of a receptor - the nicotinic acetylcholine receptor, Eur. J. Biochem. 239 (1996) 529–557.
[11] P.-J. Corringer, N.L. Novere, J.-P. Changeux, Nicotinic receptors at the amino acid level, Annu. Rev. Pharmacol. Toxicol. 40 (2000) 431–458.
[12] W. Zhong, J.P. Gallivan, Y. Zhang, L. Li, H.A. Lester, D.A. Dougherty, From ab initio quantum mechanics to molecular neurobiology: a cation–π binding site in the nicotinic receptor, Proc. Natl. Acad. Sci. USA 95 (1998) 12088–12093.
[13] V.N. Damle, A. Karlin, Effects of agonists and antagonists on the reactivity of the binding site disulfide in acetylcholine receptor from *Torpedo californica*, Biochemistry 19 (1980) 3924–3932.
[14] C. Czajkowski, A. Karlin, Structure of the nicotinic receptor acetylcholine-binding site, J. Biol. Chem. 270 (7) (1995) 3160–3164.
[15] H.R. Arias, Topology of ligand binding sites on the nicotinic acetylcholine receptor, Brain Res. Rev. 25 (1997) 133–191.
[16] C. Czajkowski, C. Kaufmann, A. Karlin, Negatively charged amino acid residues in the nicotinic receptor δ subunit that contribute to the binding of acetylcholine, Proc. Natl. Acad. Sci. USA 90 (1993) 6285–6289.
[17] D.A. Dougherty, Cation–π interactions in chemistry and biology. A new view of benzene, Phe, Tyr, and Trp, Science 271 (1996) 163–168.
[18] J.C. Ma, D.A. Dougherty, The cation–π interaction, Chem. Rev. 97 (5) (1997) 1303–1324.
[19] I. Silman, A. Karlin, Acetylcholine receptor: covalent attachment of depolarizing groups at the active site, Science 164 (1969) 1420–1421.
[20] L.D. Chabala, H.A. Lester, Activation of acetylcholine receptor channels by covalently bound agonists in cultured rat myoballs, J. Physiol. 379 (1986) 83–108.
[21] D.A. Sullivan, J.B. Cohen, Mapping the agonist binding site of the nicotinic acetylcholine receptor, J. Biol. Chem. 275 (17) (2000) 12651–12660.
[22] S.A. Robertson, J.A. Ellman, P.G. Schultz, A general and efficient route for chemical aminoacylation of transfer RNAs, J. Am. Chem. Soc. 113 (1991) 2722–2729.
[23] P.C. Kearney, N.W. Nowak, W. Zhong, S.K. Silverman, H.A. Lester, D.A. Dougherty, Dose–response relations for unnatural amino acids at the agonist binding site of the nicotinic acetylcholine receptor: tests with novel side chains and with several agonists, Mol. Pharmacol. 50 (5) (1996) 1401–1412.
[24] B. Hille, Ionic Channels of Excitable Membranes, Sinauer Associates, Inc., Sunderland, MA, 1992.
[25] G.N. Filatov, M.M. White, The role of conserved leucines in the M2 domain of acetylcholine receptor in channel gating, Mol. Pharmacol. 48 (1995) 379–384.
[26] C. Labarca, M.W. Nowak, H. Zhang, L. Tang, P. Deshpande, H.A. Lester, Channel gating governed symmetrically by conserved leucine residues in the M2 domain of nicotinic receptors, Nature 376 (1995) 514–516.

[27] G.G. Wilson, A. Karlin, The location of the gate in the acetylcholine receptor channel, Neuron 20 (1998) 1269–1281.
[28] J.L. Sussman et al., Atomic structure of acetylcholinesterase from *Torpedo californica*: A prototypic acetylcholine-binding protein, Science 253 (1991) 872–879.
[29] D.A. Dougherty, D.A. Stauffer, Acetylcholine binding by a synthetic receptor. Implications for biological recognition, Science 250 (1990) 1558–1560.
[30] M.E. Saks et al., An Engineered *Tetrahymena* $tRNA^{Gln}$ for in vivo incorporation of unnatural amino acids into proteins by nonsense suppression, J. Biol. Chem. 271 (38) (1996) 23169–23175.
[31] M. Quick, H.A. Lester, Methods for expression of excitablitity proteins in *Xenopus* oocytes, in: T. Narahashi (Ed.), Ion Channels of Excitable Cells, Academic Press, San Diego, CA, 1994, pp. 261–279.
[32] J.P. Gallivan, H.A. Lester, D.A. Dougherty, Site-specific incorporation of biotinylated amino acids as a means to identify surface exposed residues in integral membrane proteins, Chem. Biol. 4 (10) (1997) 739–749.
[33] P.M. England, Y. Zhang, D.A. Dougherty, H.A. Lester, Backbone mutations in transmembrane domains of a ligand-gated ion channel: implications for the mechanism of gating, Cell 96 (1999) 89–98.
[34] T. Ivanina, T. Peters, W.B. Thornhill, G. Levin, N. Dascal, I. Lotan, Phosphorylation by protein kinase A of RCK1 K^+ channels expressed in *Xenopus* oocytes, Biochemistry 33 (1994) 8786–8792.